ARTICLE **Open Access**

CircHIPK3 promotes colorectal cancer growth and metastasis by sponging miR-7

Kaixuan Zeng[1,2], Xiaoxiang Chen[1,2], Mu Xu[1], Xiangxiang Liu[1], Xiuxiu Hu[1], Tao Xu[1], Huiling Sun[1], Yuqin Pan[1], Bangshun He[1] and Shukui Wang[1,2]

Abstract

Mounting evidences indicate that circular RNAs (circRNAs) have a vital role in human diseases, especially cancers. More recently, circHIPK3, a particularly abundant circRNA, was proposed to be involved in tumorigenesis. However, its role in colorectal cancer (CRC) has not been explored. In this study, we found circHIPK3 was significantly upregulated in CRC tissues and cell lines, at least in part, due to c-Myb overexpression and positively correlated with metastasis and advanced clinical stage. Moreover, Cox multivariate survival analysis showed that high-level expression of circHIPK3 was an independent prognostic factor of poor overall survival (OS) in CRC (hazard ratio [HR] = 2.75, 95% confidence interval [CI] 1.74–6.51, p = 0.009). Functionally, knockdown of circHIPK3 markedly inhibited CRC cells proliferation, migration, invasion, and induced apoptosis in vitro and suppressed CRC growth and metastasis in vivo. Mechanistically, by using biotinylated-circHIPK3 probe to perform RNA pull-down assay in CRC cells, we identified miR-7 was the only one microRNA that was abundantly pulled down by circHIPK3 in both HCT116 and HT29 cells and these interactions were also confirmed by biotinylated miR-7 pull-down and dual-luciferase reporter assays. Overexpression of miR-7 mimicked the effect of circHIPK3 knockdown on CRC cells proliferation, migration, invasion, and apoptosis. Furthermore, ectopic expression of circHIPK3 effectively reversed miR-7-induced attenuation of malignant phenotypes of CRC cells by increasing the expression levels of miR-7 targeting proto-oncogenes (FAK, IGF1R, EGFR, YY1). Remarkably, the combination of circHIPK3 silencing and miR-7 overexpression gave a better effect on tumor suppression both in vitro and in vivo than did circHIPK3 knockdown or miR-7 overexpression alone. Taken together, our data indicate that circHIPK3 may have considerable potential as a prognostic biomarker in CRC, and support the notion that therapeutic targeting of the c-Myb/circHIPK3/miR-7 axis may be a promising treatment approach for CRC patients.

Introduction

Colorectal cancer (CRC) is the third most common malignant disease and the fourth most frequent cause of cancer-related death worldwide[1]. Despite many advances in the diagnosis and therapeutic improvements of this disease, the prognosis of CRC patients remains poor, owing to the late stage at initial diagnosis and high frequency of metastasis and recurrence[2]. Hence, the discovery of new potential biomarkers for prognosis predication and deeper elucidation of the exact molecular mechanisms underlying CRC malignancy may provide improved treatments of CRC patients.

Circular RNAs (circRNA) are highly conserved and stable covalently closed RNA transcripts generated by back-splicing of a single pre-mRNA with gene-regulatory potential[3,4]. Emerging evidences show that circRNAs possess closely related to human diseases, especially cancers, and may act as better biomarkers due to their abundance and stability[5,6]. Recently, circHIPK3, a particularly abundant circRNA[7,8], have been verified to be involved in metabolic dysregulation[9] and tumorigenesis[10].

Correspondence: Shukui Wang (sk_wang@njmu.edu.cn)
[1]General Clinical Research Center, Nanjing First Hospital, Nanjing Medical University, 210006 Nanjing, China
[2]School of Medicine, Southeast University, 210009 Nanjing, China
Edited by I. Amelio

SPRINGER NATURE
CDDpress

Zheng et al.[10] showed circHIPK3 was significantly upregulated in liver cancer and promoted cell proliferation, implying that circHIPK3 might be an oncogene. On the contrary, a more recent study found circHIPK3 served as a tumor suppressor to inhibit bladder cancer growth and metastasis[11]. Whether or not circHIPK3 as a suppressor gene or an oncogene still remains under debate.

MicroRNAs (miRNAs), an evolutionarily conserved group of small regulatory noncoding RNAs, have been confirmed to be involved in various biological functions[12]. Considerable studies reported that circRNAs as "miRNA sponges" to regulate gene expressions[13–17]. The most well-known circRNA is CDR1as, which harbors more than 70 selectively conserved miR-7 target sites[15,18]. However, the regulatory roles of circRNAs act as "miRNA sponges" in CRC are still largely unknown.

In this study, we identified that circHIPK3 was an oncogene, which was upregulated in CRC and increased circHIPK3 predicted poor prognosis. Furthermore, circHIPK3 could sponge endogenous miR-7 to sequester and inhibit miR-7 activity, thereby leading to increased FAK, IGF1R, EGFR, and YY1 expression. Our findings reveal a novel mechanism underlying circHIPK3 in CRC progression.

Results

CircHIPK3 is significantly upregulated in CRC and increased circHIPK3 expression predicts poor prognosis

CircHIPK3 (hsa_circ_0000284) is derived from the HIPK3 gene Exon2, whose spliced mature sequence length is 1099 bp. The result of Sanger sequencing confirmed the head-to-tail splicing in the RT-PCR product of circHIPK3 (Fig. 1a). We then evaluated the stability and localization of circHIPK3. Following Actinomycin D (an inhibitor of transcription) treatment, the half-life of circHIPK3 exceeded 24 h, while that of linear HIPK3 exhibited only about 3.8 h, indicating that circHIPK3 is highly stable (Fig. 1b). Resistance to digestion by RNase R further confirmed that circHIPK3 harbors a loop structure (Fig. 1c). Fluorescence in situ hybridization (FISH) assay showed that circHIPK3 predominately localized in the cytoplasm (Fig. 1d).

Next, we investigated the expression level of circHIPK3 in CRC cell lines and tissues. CircHIPK3 is significantly upregulated in CRC cell lines (HCT116, HT29, SW480, SW620, DLD1) compared with normal colon mucosal epithelial cell (FHC) (Fig. 1e). The similar results were also observed in CRC compared with matched normal tissues (Fig. 1f). Statistical analyses showed that increased expression of circHIPK3 was significantly associated with T status of tumor ($p = 0.028$), lymph node metastasis ($p = 0.023$), distant metastasis ($p = 0.006$), and advanced clinical stage ($p = 0.004$) (Table 1). Moreover, CRC patients with high expression of circHIPK3 had
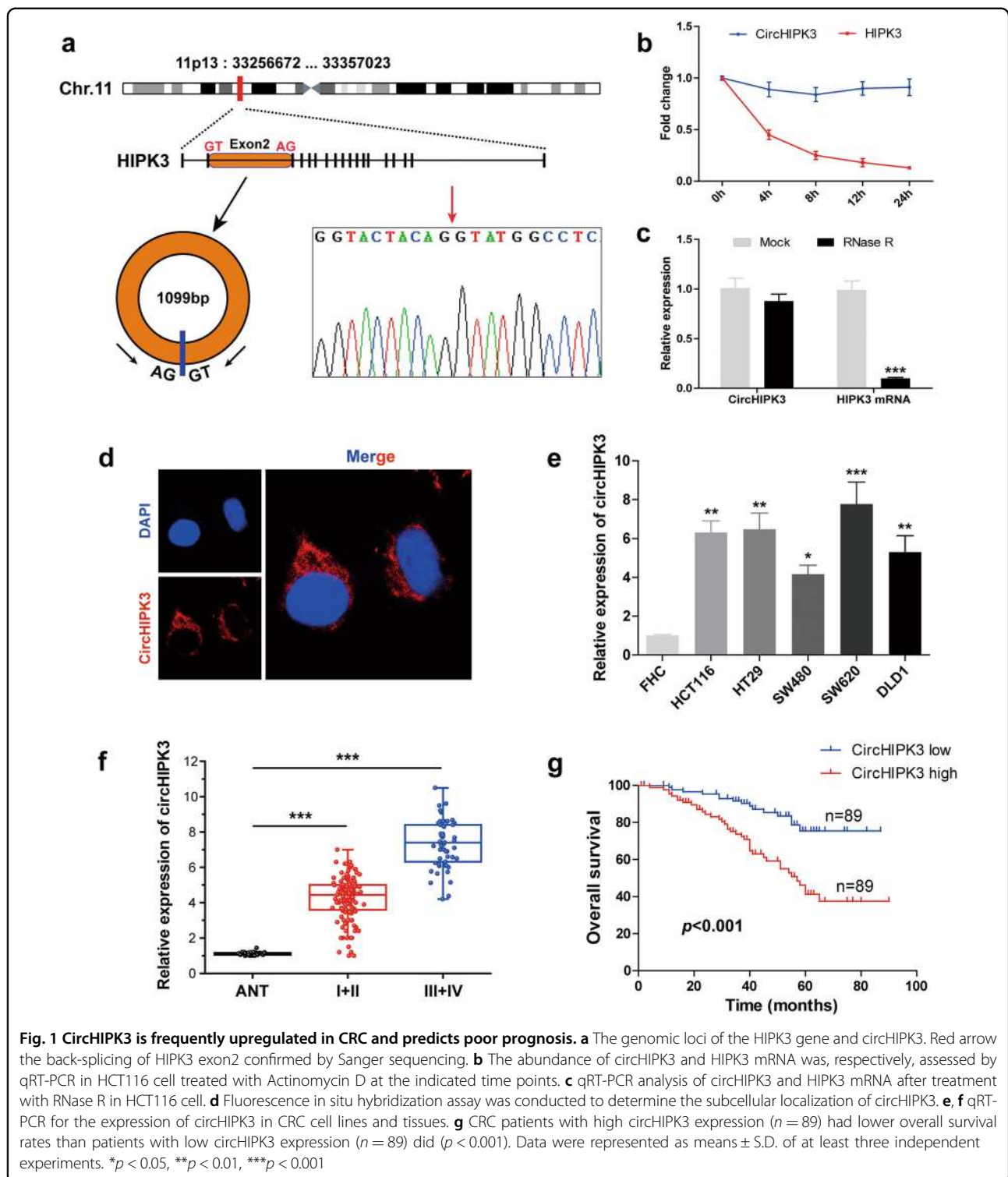
significantly shorter overall survival than those with the low expression of circHIPK3 by the analysis of Kaplan–Meier survival curve ($p < 0.001$) (Fig. 1g). Further Cox multivariate survival analysis revealed that high circHIPK3 expression was an independent prognostic factors for poor survival of CRC patients (hazard ratio [HR] = 2.75, 95% confidence interval [CI] 1.74–6.51, $p = 0.009$) (Table 2). These results suggest that circHIPK3 upregulation as an early event in CRC development and have a vital role in CRC progression.

The transcription factor c-Myb is an upstream regulator of circHIPK3 expression

Previous studies showed the enrichment for circHIPK3 transcribed by c-Myb in diabetes mellitus[9,19]. Thus, we wonder whether c-Myb can also regulate the expression of circHIPK3 in CRC. We found c-Myb was significantly overexpressed in CRC cell lines (Fig. 2a) and tissues (TCGA database) (Fig. 2b), which is consistent with previous research[20]. Then, HCT116 and HT29 cell lines were transfected with c-Myb siRNA, NC siRNA, Vector, and c-Myb, respectively. qRT-PCR results demonstrated that silencing of c-Myb decreased, but overexpression of c-Myb increased, the expression of circHIPK3 in both HCT116 and HT29 cell lines (Fig. 2c). Luciferase reporter assay showed that c-Myb overexpression noticeably enhanced the luciferase activity of the vector containing c-myb site within circHIPK3 promoter, whereas the luciferase activity of the vector with mutant c-Myb binding site was not affected (Fig. 2d). Moreover, ChIP assay also showed the amount of immunoprecipitated DNA from the circHIPK3 promoter was increased upon overexpression of c-Myb (Fig. 2e, f). Altogether, the above results indicate that c-Myb elevates the expression of circHIPK3 by directly binding to its promoter region.

Silencing of circHIPK3 inhibits CRC cells proliferation, migration, invasion, and induces apoptosis in vitro

In an attempt to investigate the biological functions of circHIPK3 in CRC, we designed three small interfering RNAs (siRNAs) targeting the junction sites of circHIPK3 to silence circHIPK3 expression in HCT116 and HT29 cell lines. These siRNAs obviously decreased circHIPK3 expression level, but had no effect on its liner isoform (Fig. 3a). And we chose si-circHIPK3#1 for the subsequent experiment due to the highest inhibitory efficiency. The colony formation assay showed that circHIPK3 knockdown significantly suppressed colony-forming ability of HCT116 and HT29 cell lines (Fig. 3b). Cell proliferation was measured by the CCK8 (Fig. 3c) and EdU assay (Fig. 3d), and silencing of circHIPK3 significantly inhibited cell proliferation in these two cell lines. In addition, more apoptotic cells are

Fig. 1 CircHIPK3 is frequently upregulated in CRC and predicts poor prognosis. a The genomic loci of the HIPK3 gene and circHIPK3. Red arrow the back-splicing of HIPK3 exon2 confirmed by Sanger sequencing. **b** The abundance of circHIPK3 and HIPK3 mRNA was, respectively, assessed by qRT-PCR in HCT116 cell treated with Actinomycin D at the indicated time points. **c** qRT-PCR analysis of circHIPK3 and HIPK3 mRNA after treatment with RNase R in HCT116 cell. **d** Fluorescence in situ hybridization assay was conducted to determine the subcellular localization of circHIPK3. **e**, **f** qRT-PCR for the expression of circHIPK3 in CRC cell lines and tissues. **g** CRC patients with high circHIPK3 expression ($n = 89$) had lower overall survival rates than patients with low circHIPK3 expression ($n = 89$) did ($p < 0.001$). Data were represented as means ± S.D. of at least three independent experiments. *$p < 0.05$, **$p < 0.01$, ***$p < 0.001$

presented in si-circHIPK3 group as compared with si-NC group in HCT116 and HT29 cell lines, respectively (Fig. 3e). Moreover, transwell invasion assay without or with matrigel demonstrated that circHIPK3 silencing markedly impeded HCT116 and HT29 cells migration (Fig. 3f) and invasion (Fig. 3g) by 46% and 51%, respectively. These data collectively indicate that silencing of circHIPK3 can retard the progression of CRC cells.

Table 1 Correlations between circHIPK3 expression and clinical characteristics in CRC patients ($n = 178$)

Clinicopathologic parameters	Total ($n = 178$)	CircHIPK3 expression[a]		p value
		Low (%)	High (%)	
Age (years)				
≤65	79	41 (51.9%)	38 (48.1%)	0.763
>65	99	48 (48.5%)	51 (51.5%)	
Gender				
Male	102	49 (48.0%)	53 (52.0%)	0.650
Female	76	40 (52.6%)	36 (47.4%)	
Tumor site				
Colon	115	62 (53.9%)	53 (46.1%)	0.210
Rectum	63	27 (42.8%)	36 (57.2%)	
Tumor size (cm)				
≤5	107	57 (53.3%)	50 (46.7%)	0.358
>5	71	32 (45.1%)	39 (54.9%)	
Pathological T category				
T1–T2	48	31 (64.6%)	17 (35.4%)	0.028*
T3–T4	130	58 (44.6%)	72 (55.4%)	
Lymph node metastasis				
N0	102	59 (57.8%)	43 (42.2%)	0.023*
N1–2	76	30 (39.5%)	46 (60.5%)	
Distant metastasis				
M0	155	84 (54.2%)	71 (45.8%)	0.006**
M1	23	5 (21.7%)	18 (78.3%)	
TNM stage				
I–II	121	70 (57.8%)	51 (42.2%)	0.004**
III–IV	57	19 (33.3%)	38 (66.7%)	
Differentiation				
Well	23	12 (52.2%)	11 (47.8%)	0.695
Moderate	129	66 (51.1%)	63 (48.9%)	
Poor	26	11 (42.3%)	15 (57.7%)	

*$p < 0.05$
**$p < 0.01$
[a]Using median circHIPK3 values as cutoff

CircHIPK3 can sponge miR-7 in CRC cell lines

To explore whether circHIPK3 can function as "miRNA sponge" in CRC cells, we selected the top ten (miR-599, miR-93-3p, miR-365a-5p, miR-365b-5p, miR-421, miR-570-3p, miR-597-5p, miR-7, miR-1207-3p, miR-124-5p) candidate miRNAs through CircNet database[21]. A 3′ terminal-biotinylated-circHIPK3 probe was designed to determine which miRNAs potentially interact with circHIPK3. The probe was verified to pull-down circHIPK3 in CRC cells and circHIPK3 overexpression increased the pull-down efficiency (Fig. 4a). qRT-PCR analyses revealed that miR-7 was the only one miRNA that was abundantly pulled down by circHIPK3 probe in both HCT116 and HT29 cells (Fig. 4b and c). To further consolidate the direct binding of miR-7 and circHIPK3, we utilized biotin-labeled miR-7 and its mutant mimics to pull-down circHIPK3 in HCT116 and HT29 cells with circHIPK3 overexpression, the results showed wild-type miR-7 captured more circHIPK3 compared with the mutant (Fig. 4d). Next, we carried out luciferase reporter assays and demonstrated that overexpression of miR-7 significantly decreased the luciferase activity of the vector containing the complete circHIPK3 sequence, but did not affect the luciferase activity of the vector with mutant miR-7-binding site in HCT116 and HT29 cells (Fig. 4e). Furthermore, we applied FISH to assess whether there is a co-location between circHIPK3 and miR-7, the result showed that circHIPK3 and miR-7 were co-localized in cytoplasm (Fig. 4f).

We then evaluated the expression of miR-7 in CRC tissues, qRT-PCR result showed miR-7 was significantly downregulated with the increasing of clinical stages (Fig. 4g). And overexpression of circHIPK3 decreased, but silencing of circHIPK3 increased, the expression of miR-7 in HCT116 and HT29 cell lines (Fig. 4h). Moreover, circHIPK3 expression was negatively correlated with the expression of miR-7 in CRC tissues ($r = -0.453$, $p < 0.001$) (Fig. 4i). Taken together, these data demonstrate that circHIPK3 acts as a miRNA sponge for miR-7 in CRC.

Overexpression of circHIPK3 effectively reverses miR-7-induced inhibition of CRC cells progression

MiR-7, a well-known tumor suppressor, was involved in many human tumors development and progression[22–25], including CRC[26]. Our data also showed that overexpression of miR-7 significantly suppressed CRC cells proliferation, migration, invasion and induced apoptosis (Fig. 5a–e) resembling that of circHIPK3 silencing (Supplementary Fig. 1a–c). We then investigated whether circHIPK3 exerted tumor-promoting effect by sponge activity of miR-7, HCT116, and HT29 cells were co-transfected with miR-7 mimics and circHIPK3 expression vectors. The colony formation assay showed that CRC cells co-transfected with circHIPK3 plasmids and miR-7 mimics exhibited more cloned cells compared with the cells transfected with miR-7 mimics alone (Fig. 5a). EdU incorporation assay indicated ectopically overexpressed miR-7 together with circHIPK3 promoted CRC cells proliferation compared with miR-7 overexpression alone (Fig. 5b). Furthermore, less apoptotic cells were showed in miR7 + circHIPK3 group as compared with miR7 group

Table 2 Univariate and multivariate overall survival analysis of prognostic factors for CRC patients ($n = 178$)

Clinicopathologic Parameters	Overall survival					
	Univariate analysis			Multivariate analysis		
	HR	95% CI	*p* value	HR	95% CI	*p* value
Age (≤65 years vs >65 years)	0.94	0.64–2.26	0.586			
Gender (male vs female)	1.09	0.71–2.01	0.635			
Tumor site (colon vs rectum)	1.15	0.51–1.89	0.257			
Tumor size (≤5 cm vs >5 cm)	2.17	0.87–4.12	0.128			
Tumor infiltration (T1–T2 vs T3–T4)	2.48	1.16–5.41	0.041*	1.87	0.58–3.14	0.367
Lymph node metastasis (N0 vs N1–2)	3.11	1.97–5.82	0.012*	1.42	0.69–2.86	0.159
Distant metastasis (M0 vs M1)	3.79	1.82–6.87	0.026*	2.24	1.16–4.75	0.044*
TNM stage (I–II vs III–IV)	5.12	2.07–8.67	<0.001***	3.62	1.31–8.87	0.002**
Differentiation (well/moderate vs poor)	1.04	0.52–4.12	0.324			
CircHIPK3 expression (low vs high)[a]	4.12	1.97–7.96	<0.001***	2.75	1.74–6.51	0.009**

*$p < 0.05$
**$p < 0.01$
***$p < 0.001$
[a]Using median circHIPK3 values as cutoff

(Fig. 5c). Likewise, transwell invasion assay without or with matrigel reveled that miR-7 together with circHIPK3 overexpression obviously impeded HCT116 and HT29 cells migration (Fig. 5d) and invasion (Fig. 5e) compared with miR-7 overexpression alone. In addition, we also found that overexpression of miR-7 combined with knockdown of circHIPK3 displayed an additive suppressive effect on CRC cell malignant phenotype compared with miR-7 overexpression or circHIPK3 silencing alone (Supplementary Fig. 1a–c).

Accumulating evidence indicated that miR-7 could simultaneously target various oncogenes involved in diverse signaling pathways in different human tumors[27]. We then wonder whether circHIPK3 exert pro-tumor role by elevating the expression of miR-7 targeting oncogenes. A panel of growth and metastasis-related miR-7 targets was chosen for qRT-PCR analysis. The results showed that circHIPK3 status affected the expression of FAK, IGF1R, EGFR, and YY1, but not that of PAX6, XRCC2, and RAF1. Ectopic expression of circHIPK3 increased, but knockdown of circHIPK3 decreased, the expression levels of FAK, IGF1R, EGFR, and YY1 (Fig. 5f). Moreover, the expression of FAK, IGF1R, EGFR, and YY1 was markedly increased in CRC cells (HCT116 and HT29) co-transfected with miR-7 mimics and circHIPK3 vectors compared with the cells transfected with miR-7 mimics alone (Fig. 5g). These above results implicate that overexpression of circHIPK3 effectively reverses miR-7-induced attenuation of aggressive phenotypes of CRC cells by sponging miR-7 and subsequent promotion of FAK, IGF1R, EGFR, and YY1 expression.

Silencing of circHIPK3 combined with overexpression of miR-7 exhibits an additive inhibitory effect on CRC growth and metastasis in xenograft animal models

To further assess whether circHIPK3 exerts tumor-promoting effect in vivo, we established the xenograft mouse models by subcutaneously injecting equal amount of HCT116 cells ($n = 8$ for each group). After ~10 days, when the volume of the tumor reached about 100 mm^3, si-circHIPK3 alone, agomir-7 alone or both were injected intratumorally every two days for two weeks. As shown in Fig. 6a, intratumorally injection of agomir-7 or si-circHIPK3 markedly reduced tumor volume and weight, respectively. More importantly, the combined si-circHIPK3 and agomir-7 group displayed less tumor volume and weight than that of si-circHIPK3 or agomir-7 alone (Fig. 6a). Likewise, miR-7 overexpression or circHIPK3 knockdown significantly decreased the expression of miR-7 targeting proto-oncogenes (FAK, IGF1R, EGFR, YY1) both at the mRNA and protein levels, and the combined group exhibited less expression of these oncogenes (Supplementary Fig. 2a, b). IHC analysis also showed that decreased Ki67, MMP9-positive cells, and microvascular density, and increased cleaved caspase-3-positive cells in si-circHIPK3 + agomir-7 group compared with si-circHIPK3 or agomir-7 group alone (Fig. 6b).

We also established the metastasis models through tail-vein injecting HCT116 cells into nude mice ($n = 8$ for
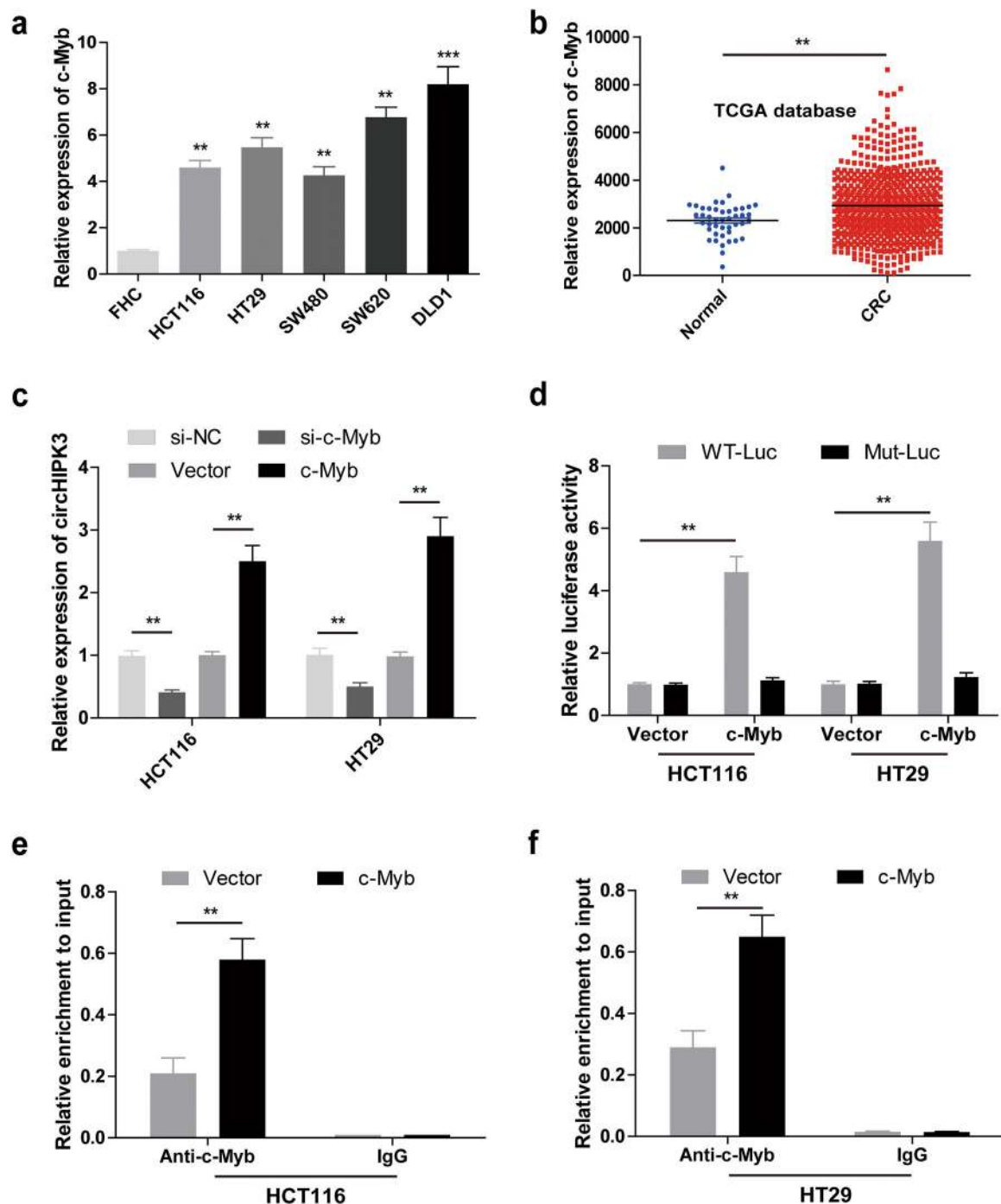
Fig. 2 The transcription factor c-Myb transcriptionally elevates circHIPK3 in CRC cell lines. a, b qRT-PCR for the expression of c-Myb in CRC cell lines and tissues (TCGA RNA-seq database). **c** qRT-PCR analysis of the expression of circHIPK3 in HCT116 and HT29 cell lines with c-Myb knockdown or overexpression. **d** Luciferase activity analysis in HCT116 and HT29 cells co-transfected with the pGL3-basic-circHIPK3-wt/mut vectors, pcDNA3.1-c-Myb vectors and pRL-TK. **e, f** ChIP-qPCR was performed in HCT116 and HT29 cells to identify circHIPK3 as a direct binding target of c-Myb. Mouse IgG was used as a negative control. Data were represented as means ± S.D. of at least three independent experiments. **$p < 0.01$, ***$p < 0.001$

each group). As illustrated in Fig. 6c, an average of 38 lung metastatic nodules per mice was observed in control group and 17, 19 were respectively observed in agomir-7 or si-circHIPK3 group, whereas only 6 were observed in the combined si-circHIPK3 and agomir-7 group. Overall, these data indicate that silencing of circHIPK3 suppresses
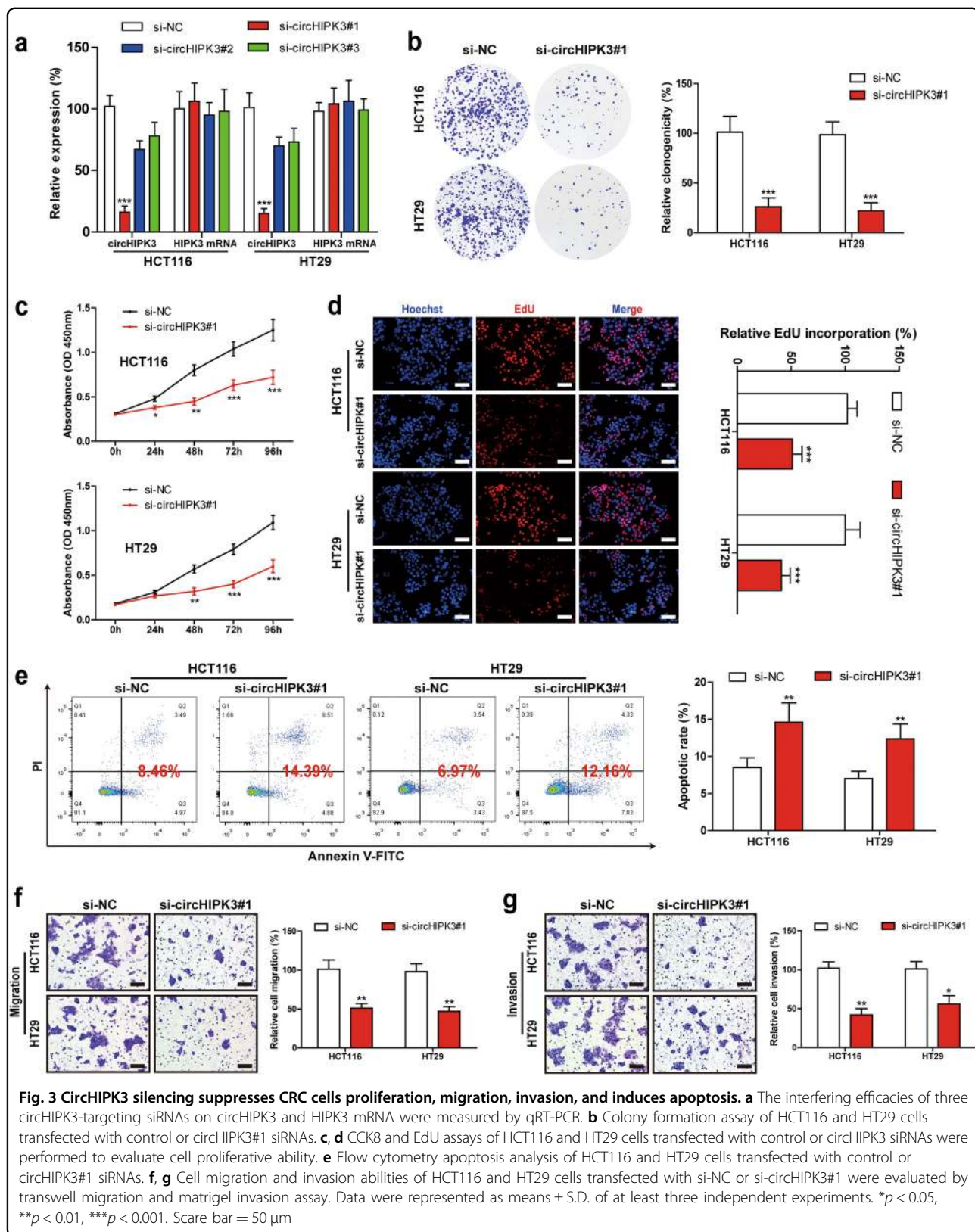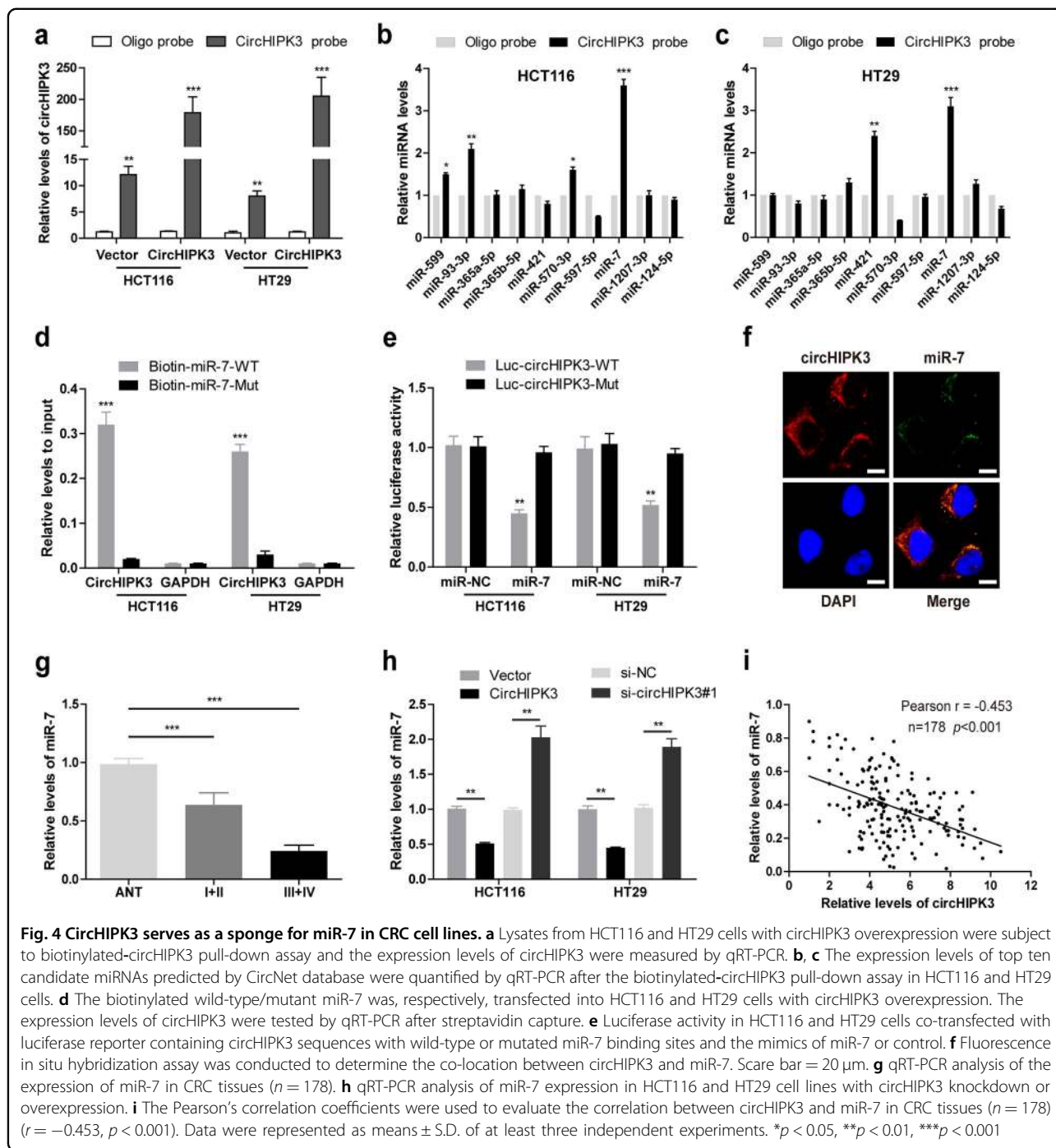
Fig. 3 CircHIPK3 silencing suppresses CRC cells proliferation, migration, invasion, and induces apoptosis. a The interfering efficacies of three circHIPK3-targeting siRNAs on circHIPK3 and HIPK3 mRNA were measured by qRT-PCR. **b** Colony formation assay of HCT116 and HT29 cells transfected with control or circHIPK3#1 siRNAs. **c**, **d** CCK8 and EdU assays of HCT116 and HT29 cells transfected with control or circHIPK3 siRNAs were performed to evaluate cell proliferative ability. **e** Flow cytometry apoptosis analysis of HCT116 and HT29 cells transfected with control or circHIPK3#1 siRNAs. **f**, **g** Cell migration and invasion abilities of HCT116 and HT29 cells transfected with si-NC or si-circHIPK3#1 were evaluated by transwell migration and matrigel invasion assay. Data were represented as means ± S.D. of at least three independent experiments. $*p < 0.05$, $**p < 0.01$, $***p < 0.001$. Scare bar = 50 μm

Fig. 4 CircHIPK3 serves as a sponge for miR-7 in CRC cell lines. a Lysates from HCT116 and HT29 cells with circHIPK3 overexpression were subject to biotinylated-circHIPK3 pull-down assay and the expression levels of circHIPK3 were measured by qRT-PCR. **b**, **c** The expression levels of top ten candidate miRNAs predicted by CircNet database were quantified by qRT-PCR after the biotinylated-circHIPK3 pull-down assay in HCT116 and HT29 cells. **d** The biotinylated wild-type/mutant miR-7 was, respectively, transfected into HCT116 and HT29 cells with circHIPK3 overexpression. The expression levels of circHIPK3 were tested by qRT-PCR after streptavidin capture. **e** Luciferase activity in HCT116 and HT29 cells co-transfected with luciferase reporter containing circHIPK3 sequences with wild-type or mutated miR-7 binding sites and the mimics of miR-7 or control. **f** Fluorescence in situ hybridization assay was conducted to determine the co-location between circHIPK3 and miR-7. Scare bar = 20 μm. **g** qRT-PCR analysis of the expression of miR-7 in CRC tissues (n = 178). **h** qRT-PCR analysis of miR-7 expression in HCT116 and HT29 cell lines with circHIPK3 knockdown or overexpression. **i** The Pearson's correlation coefficients were used to evaluate the correlation between circHIPK3 and miR-7 in CRC tissues (n = 178) (r = −0.453, p < 0.001). Data were represented as means ± S.D. of at least three independent experiments. *p < 0.05, **p < 0.01, ***p < 0.001

CRC growth and metastasis in vivo and combined with miR-7 overexpression exhibits an additive effect on tumor repression.

Discussion

It is becoming increasingly clear that circRNAs have a crucial role in cancer development and progression and affect the hallmarks of cancer[28,29]. However, their roles in CRC remain largely unknown. In this study, we found

circHIPK3 was significantly upregulated in CRC, at least in part, due to c-Myb overexpression and increased circHIPK3 predicted poor prognosis. Mechanistically, ectopic expression of circHIPK3 could rescue the expression of miR-7 targeting oncogenes by sponging miR-7, thereby promoting CRC progression (Fig. 7). Moreover, the combination of circHIPK3 knockdown and miR-7 overexpression gave a better tumor-suppressive effect both in vitro and in vivo than did circHIPK3 silencing or miR-7
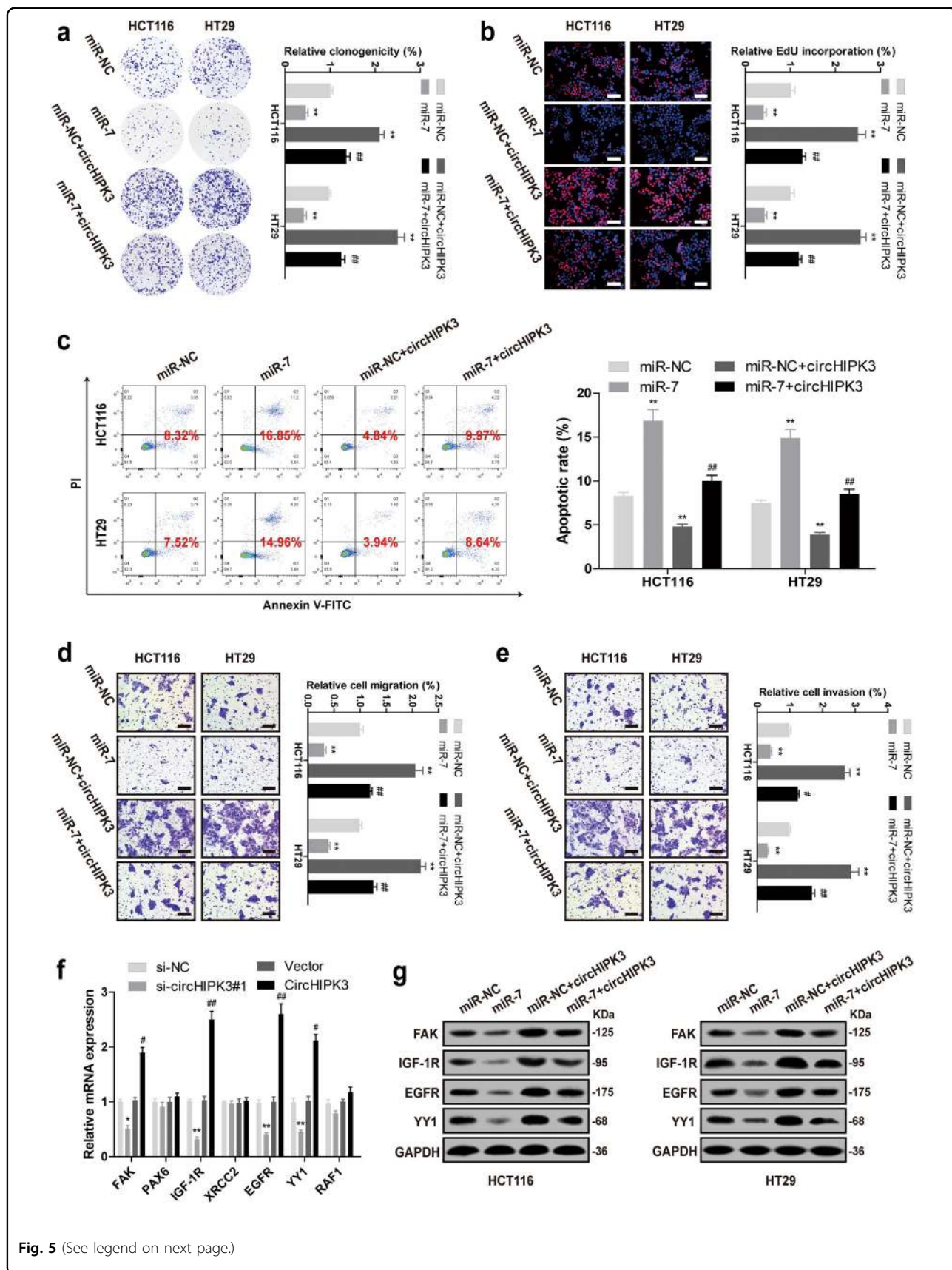
Fig. 5 (See legend on next page.)

(see figure on previous page)

Fig. 5 Overexpression of circHIPK3 effectively reverses miR-7-induced inhibition of CRC cells progression. HCT116 and HT29 cells transfected with miR-control, miR-7, circHIPK3, or miR-7 + circHIPK3. Then the ability of cell cloning, proliferation, migration and invasion was, respectively, assessed by colony formation assay (**a**), EdU assay (**b**), transwell migration (**d**), and matrigel invasion (**e**) assay. And cell apoptosis analysis was tested by flow cytometry with Annexin V-FITC/PI double staining (**c**). * vs control group, # vs mir-7 group. **f** qRT-PCR analysis of the expression of growth and metastasis-related miR-7 targets in HCT116 and HT29 cells with circHIPK3 knockdown or overexpression. * vs si-NC group, # vs vector group. **g** Western blot analysis of the protein expression of FAK, IGF1R, EGFR, and YY1 in fore-mentioned four groups in HCT116 and HT29 cells. Data were represented as means ± S.D. of at least three independent experiments. *$p < 0.05$, **$p < 0.01$; #$p < 0.05$, ##$p < 0.01$. Scare bar = 50 μm

reintroduction alone. Thus, our study demonstrate that co-expressing miR-7 along with a circHIPK3 inhibitor may be a promising treatment approach for patients with CRC.

Previous studies indicated the enrichment for circHIPK3 transcribed by c-Myb in diabetes mellitus[9,19]. c-Myb overexpression occurring in many malignancies, including CRC, often marks poor prognosis[30]. And c-Myb have a pivotal role in promoting cell proliferation, survival, and metastasis by activating various signaling pathways[31]. We evaluated whether proto-oncogene c-Myb also regulated circHIPK3 expression in CRC. Luciferase reporter assay displayed that overexpression of c-Myb promoted the transcription of circHIPK3, and ChIP-qPCR analysis further confirmed c-Myb could directly bind to circHIPK3 promoter region in CRC cells. These indicated that transcription factor c-Myb is an upstream regulator of circHIPK3 expression, which were consistent with the previous reports.
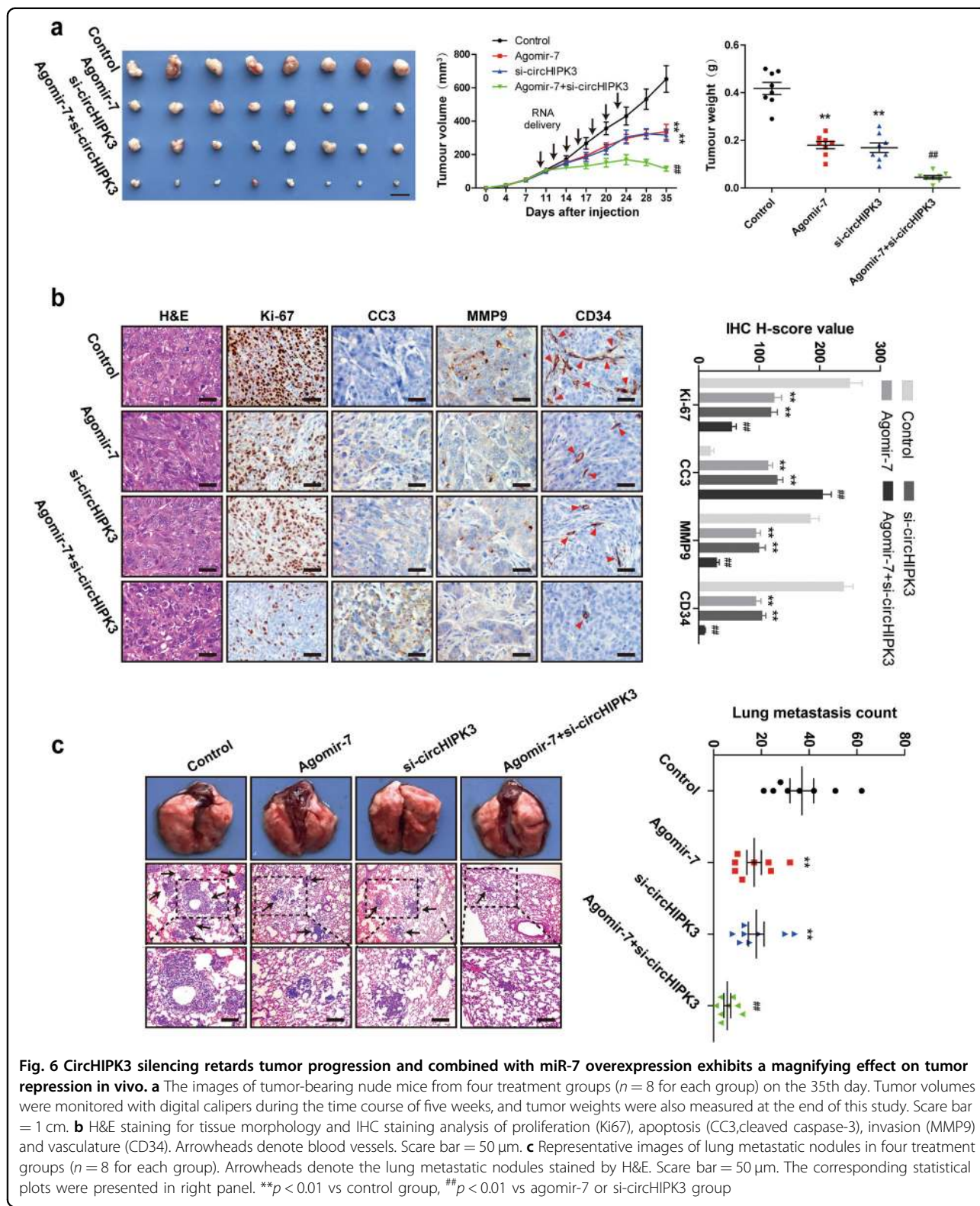
Emerging studies show that circRNAs are abundant in the human transcriptome[7,15,18]. In addition, circRNAs are more stable than other types of RNA because of their covalently closed structures. Therefore, circRNAs are more suitable as potential cancer biomarkers than other RNAs, such as miRNAs and lncRNAs, due to their abundance and stability. As expected, there are already many circRNAs recognized as cancer biomarkers. CiRS-7, circPVT1, circBRAF, circPRDM2, and circTCF25 was respectively identified to be a promising prognostic biomarker in colorectal cancer[6], gastric cancer[5], glioma[32], hepatocellular carcinoma[33], and bladder cancer[34]. Herein, we found circHIPK3 was frequently upregulated in CRC and patients with circHIPK3 high expression had significantly shorter overall survival than those with the low expression of circHIPK3, implying that circHIPK3 might be a promising prognostic biomarker in CRC.
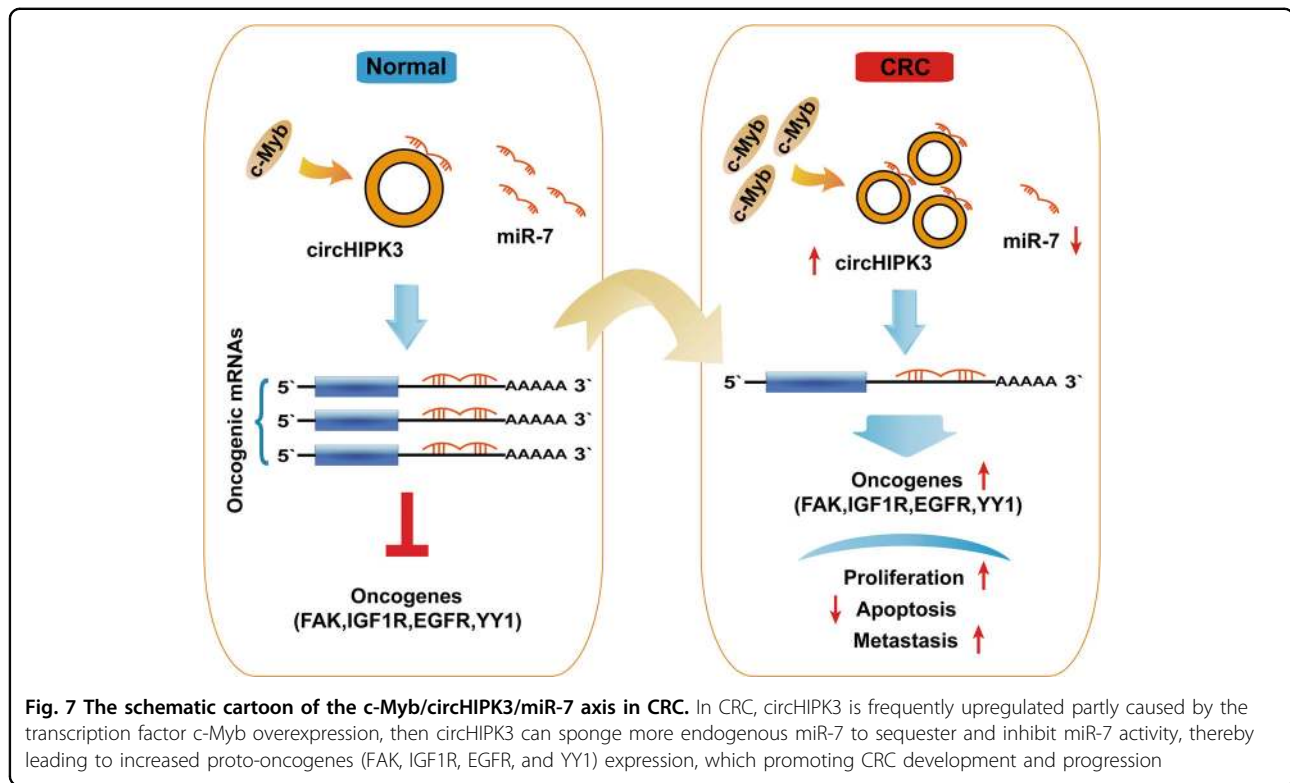
Up to now, numerous studies have shown that circRNAs exerted various biological functions by acting as competing endogenous RNAs (ceRNAs)[13,35,36]. Analogously, circHIPK3 could promote cell growth by sponging miR-124[10]. However, Shan et al.[9] reported that circHIPK3 controlled diabetic proliferative retinopathy via sponging miR-30a, but not miR-124. Meanwhile, circHIPK3 was proposed to inhibit bladder cancer progression through sponging miR-558[11]. One likely explanation for these discrepancies is that circRNA have its biological roles in tissue/developmental-stage specific context[4]. Importantly, we identified that circHIPK3 could interact with miR-7 in CRC by biotinylated RNA pull-down and dual-luciferase reporter assays, which has not been reported by previous studies.

MiR-7, a well-known tumor suppressor, was proposed to participate in the development and progression of different types of human cancers[37]. In agreement with previous studies, our data indicated that miR-7 overexpression significantly inhibited CRC cells proliferation, migration, invasion and induced apoptosis, and these inhibitory effects were exceedingly similar to circHIPK3 silencing. Moreover, we found circHIPK3 could sponge endogenous miR-7 to sequester and reduce miR-7 activity, thus resulting in increasing the expression of miR-7 targeting oncogenes (FAK, IGF1R, EGFR, and YY1). FAK—a kinase regulated by cell–ECM interactions and known to be important for cellular migration, which promoted tumor invasion and metastasis by elevating the expression of VEGF, MMP2, and MMP9[38]. Wealth of studies confirmed that IGF1R and EGFR could respectively activate PI3K/AKT and MEK/ERK signaling pathways to promote cancer progression and drug resistance[39,40]. And we also found that inhibition of circHIPK3 could reverse CRC cell resistance to EGFR inhibitor cetuximab (data not shown). Besides, YY1 was reported to promote cancer growth through inhibiting p53 and activating Wnt signaling pathways[40]. These oncogenes were frequently overexpressed in CRC and our data showed that circHIPK3 upregulated these proto-oncogenes expression to promote CRC progression, suggesting that circHIPK3 was an oncogene in CRC. Further studies will be required to investigate the role of circHIPK3 in other malignances.

In summary, our findings provide robust evidence that c-Myb transcriptionally elevates circHIPK3 and circHIPK3 serves as a novel oncogenic circRNA by sponging miR-7, as well as a promising prognostic biomarker in CRC. Our data also suggest that targeting

Fig. 6 CircHIPK3 silencing retards tumor progression and combined with miR-7 overexpression exhibits a magnifying effect on tumor repression in vivo. a The images of tumor-bearing nude mice from four treatment groups (*n* = 8 for each group) on the 35th day. Tumor volumes were monitored with digital calipers during the time course of five weeks, and tumor weights were also measured at the end of this study. Scare bar = 1 cm. **b** H&E staining for tissue morphology and IHC staining analysis of proliferation (Ki67), apoptosis (CC3,cleaved caspase-3), invasion (MMP9) and vasculature (CD34). Arrowheads denote blood vessels. Scare bar = 50 μm. **c** Representative images of lung metastatic nodules in four treatment groups (*n* = 8 for each group). Arrowheads denote the lung metastatic nodules stained by H&E. Scare bar = 50 μm. The corresponding statistical plots were presented in right panel. **p < 0.01 vs control group, ##p < 0.01 vs agomir-7 or si-circHIPK3 group

Fig. 7 The schematic cartoon of the c-Myb/circHIPK3/miR-7 axis in CRC. In CRC, circHIPK3 is frequently upregulated partly caused by the transcription factor c-Myb overexpression, then circHIPK3 can sponge more endogenous miR-7 to sequester and inhibit miR-7 activity, thereby leading to increased proto-oncogenes (FAK, IGF1R, EGFR, and YY1) expression, which promoting CRC development and progression

the c-Myb/circHIPK3/miR-7 axis as a potential treatment strategy for fighting CRC.

Materials and methods

Cell cultures and patient tissues

Human normal colon epithelial cell (FHC) and color-ectal cancer cell lines (HCT116, HT29, SW480, SW620, DLD1) were purchased from American Type Culture Collection (Manassas, VA, USA) and were cultured in Dulbecco's modified Eagle's medium (DMEM) supple-mented with 10% fetal bovine serum (Gibco, Vienna, Austria). Cells in this medium were placed in a humidified atmosphere of 5% CO_2 at 37 °C. All cell lines were free of mycoplasma contamination.

The 178 samples of CRC and 40 adjacent normal for-malin-fixed, paraffin-embedded (FFPE) tissues were obtained from patients during operation at Affiliated Nanjing First Hospital of Nanjing Medical University (Nanjing, China). The patient characteristics were showed in Table 1. None of these patients received preoperative chemotherapy or radiotherapy. This study was approved by the ethics committee of Nanjing First Hospital and written informed consent was obtained from each patient.

Quantitative reverse transcription polymerase reaction (qRT-PCR)

Total RNA was extracted from tissues and cells by using TRIzol reagent (Invitrogen, CA, USA). For miRNA, the expression was determined by stem-loop primer SYBR Green quantitive real time-PCR (RiboBio, Guangzhou, China). For circRNA and mRNA, Total RNA was reverse transcribed to cDNA and then qPCR was conducted by using a SYBR Green PCR Kit (Takara, Otsu, Japan). All primer sequences were designed and synthesized by RiboBio (Guangzhou, China). GAPDH was chosen as the reference gene for circRNA and mRNA. U6 was chosen as an internal control for miRNA. Gene expression was quantified using the $2^{-\Delta\Delta Ct}$ method.

Actinomycin D and RNase R treatment

The culture medium was added to Actinomycin D (2 mg/ml) or DMSO (SigmaeAldrich, St. Louis, MO,USA) to assess the stability of circHIPK3 and its linear isoform. Total RNA (10 μg) was incubated with 40U RNase R (Epicentre Technologies, Madison, WI, USA) at 37 °C for 60 min. After treatment with Actinomycin D and RNase R, the expression levels of HIPK3 and circHIPK3 were determined by qRT-PCR.

Oligonucleotide transfection

si-circHIPK3, si-c-Myb, miR-7 mimics, and their respective control oligonucleotides were synthesized by Gene-Pharma (Shanghai, China). Transfections were performed with final concentrations of 50 nM of miRNA mimics and siRNAs using the Lipofectamine 2000 reagent (Invitrogen) according to the manufacturer's protocol.

Plasmids construction and stable transfection

The method of constructing stable circHIPK3 or c-Myb overexpression cell lines has been described in the previous study[11]. In brief, human circHIPK3 and c-Myb cDNA was synthesized and cloned into pcD-ciR and pcDNA3.1 vector (Geenseed Biotech, Guangzhou, China), respectively. Then, HCT116 and HT29 cells were transfected with these plasmids, followed by selected with G418.

Luciferase reporter assay

For the promoter of circHIPK3 luciferase reporter assay, the wild-type and mutant promoters of circHIPK3 were synthesized and inserted into pGL3-basic vectors (Gene-Creat, Wuhan, China), then the pGL3-basic-circHIPK3-wt/mut vectors and pcDNA3.1-c-Myb vectors were co-transfected with pRL-TK into HCT116 and HT29 cells using Lipofectamine 2000 reagent. For circHIPK3 and miR-7 luciferase reporter assay, the circHIPK3 sequences containing wild-type or mutated miR-7 binding sites were respectively synthesized and inserted into pmirGLO luciferase vector (GeneCreat, Wuhan, China), and then co-transfected with miR-7 mimics into HCT116 and HT29 cell lines were accomplished using Lipofectamine 2000. Cells were harvested at 48 h after transfection and luciferase activity was detected by the dual-luciferase reporter assay system (Promega). Relative luciferase activity was normalized to the Renilla luciferase internal control.

Chromatin immunoprecipitation assay

Chromatin immunoprecipitation (ChIP) assay was conducted using the ChIP Assay Kit (Beyotime, Shanghai, China) according to the manufacturer's guidelines with slight modifications. In brief, HCT116 and HT29 cells were treated with 1% formaldehyde for 10 min and quenched with 0.125 M glycine. Then the lysate was immunoprecipitated with anti-c-Myb (sc-74512, Santa Cruz) or normal mouse IgG antibody. Immunoprecipitated DNA was analyzed by qPCR.

Colony formation assay

Twenty-four hours after transfection, 500 HCT116 and HT29 cells were initially seeded into 6-well plates and cultured routinely for two weeks. Then the colonies were fixed with methanol for 10 min and stained with 0.1% crystal violet for 15 min at room temperature. Cell colonies were counted and photographed.

Cell counting kit-8 proliferation assay

The CCK8 assay was performed to assess CRC cells proliferative ability according to the manufacturer's instruction (Dojindo Laboratories, Kumamoto, Japan). HCT116 and HT29 cells (1×10^3) were plated in 96-well plates and treated with 10 μl of CCK8 solution, then the spectrophotometrically at 450 nM was analyzed by automatic microplate reader (Synergy4; BioTek, Winooski, VT, USA).

5-Ethynyl-20-deoxyuridine (EdU) incorporation assay

The EdU assay was performed with a Cell-Light EdU DNA Cell Proliferation Kit (RiboBio, Guangzhou, China) according to the manufacturer's protocol. After incubation with 50 mM EdU for 2 h, the HCT116 and HT29 cells were fixed in 4% paraformaldehyde and stained with Apollo Dye Solution for proliferating cells, followed by mounted with Hoechst 33342. Then the EdU-positive cells were photographed and counted under an Olympus FSX100 microscope (Olympus, Tokyo, Japan) in five randomly selected fields.

Apoptosis analysis

Cell apoptosis was analyzed using the Annexin V-FITC/Propidium Iodide (PI) Apoptosis Detection Kit (BD Biosciences #556547) according to the manufacturer's instruction. HCT116 and HT29 cells were stained with FITC and PI and then analyzed by fluorescence-activated cell sorting using FACScan (BD Biosciences, San Jose, CA, USA). The cell apoptosis data were analyzed by Flowjo V10 software (Tree Star, San Francisco, CA, USA).

Transwell migration and invasion assays

The cell migration and invasion assays were conducted by using transwell chamber (Corning, NY, USA), which was coated with (invasion assay) or without (migration assay) the matrigel mix (BD Biosciences, San Jose, CA, USA) according to the manufacturer's protocol. After incubation for 24 h, the cells located on the upper surfaces of the transwell chambers were scraped with cotton swabs and the cells located on the lower surfaces were fixed with methanol for 10 min, followed by stained with crystal violet. Then the stained cells were photographed and counted in five randomly selected fields.

RNA fluorescence in situ hybridization

The RNA fluorescence in situ hybridization assay was performed by using Fluorescent In Situ Hybridization Kit (RiboBio, Guangzhou, China) according to the manufacturer's guidelines. And Cy3-labeled circHIPK3 probes and Dig-labeled locked nucleic acid miR-7 probes (Ribo-Bio, Guangzhou, China) were measured by the Fluorescent In Situ Hybridization Kit, followed by visualized with a confocal microscopy.

Biotinylated RNA pull-down assay

The pull-down assay with biotinylated RNA was performed as described[11,41]. In brief, for circHIPK3 pulled down miRNAs, the biotinylated-circHIPK3 probe was

incubated with C-1 magnetic beads (Life Technologies, Carlsbad, CA, USA) to generate probe-coated beads, then incubated with sonicated HCT116 and HT29 cells at 4 °C overnight, followed by eluted and qRT-PCR. For miR-7 pulled down circHIPK3, HCT116 and HT29 cells with circHIPK3 overexpression were transfected with biotinylated miR-7 mimics or mutant using Lipofectamine 2000. The cells were harvested, lysed, sonicated, and incubated with C-1 magnetic beads (Life Technologies, Carlsbad, CA, USA), followed by washed and qRT-PCR.

Western blotting

The HCT116 and HT29 cells were lysed in RIPA lysis buffer. Then, equal amounts of protein were resolved by SDS-PAGE analysis and electrotransferred onto a PVDF membrane (Millipore, Schwalbach, Germany), then blocked with 5% skim milk powder and incubated with primary antibody at 4 °C overnight. The primary antibodies used were anti-FAK (#3285, Cell Signaling Technology), anti-IGF1R (#ab39675, Abcam), anti-EGFR (#4267, Cell Signaling Technology), anti-YY1 (#66281-1-Ig, Proteintech), anti-GAPDH (#ab181602, Abcam). Then the membranes were incubated with HRP-conjugated secondary antibody for 1 h at room temperature, the blots were visualized using an enhanced chemiluminescence kit (Pierce, Waltham, MA, USA).

Immunohistochemistry (IHC)

IHC was performed on formalin-fixed, paraffin-embedded tissue sections as described previously[42]. Primary antibodies against Ki67 (#ab15580, Abcam), cleaved caspase-3 (#ab2302, Abcam), MMP9 (#ab38898, Abcam), and CD34 (#ab81289, Abcam) were used. The complex was visualized with DAB complex, and the nuclei were counterstained with haematoxylin. All sections were scored by the semi-quantitative H-score approach[42] and validated by two experienced pathologists.

Animal experiments

For xenograft tumor model, 5-week-old male BALB/c nude mice were randomly divided into four groups ($n = 8$ for each group). HCT116 (5×10^6/0.2 ml PBS) cells were subcutaneously inoculated into the right flank of each nude mice. Tumor volumes were measured every 3 days with digital calipers and were calculated by the following formula: tumor volume = 1/2 (length × width^2). After ~10 days, when the volume of the tumor reached about 100mm^3, cholesterol-conjugated si-circHIPK3 alone, agomir-7 alone or both (10 nM) (Gene-Pharma, Shanghai, China) in 0.1 ml of saline buffer were locally injected into the tumor mass, respectively. The injections were performed seven times at an interval of two days between each injection (i.e., day 10, 12, 14…). Thirty-five days later,

the mice were killed and the volume and weight of the tumors were measured. Then the tumor tissues were harvested for use in further hematoxylin and eosin (H&E) and IHC staining.

For metastasis assay, HCT116 (1×10^6/ 0.2 ml PBS) cells with corresponding treatment were tail-vein injected into 32 five-week-old male BALB/c nude mice which were randomly divided into six groups ($n = 8$ for each group). Seven weeks later, the mice were killed, and all the lungs are surgically removed and the number of macroscopically visible pulmonary metastases nodules per mouse was counted by two experienced pathologists. Then the lung tissues were fixed in 10% neutral phosphate-buffered formalin, followed by HE staining. The animal experiments were approved by the Animal Care Committee of Nanjing Medical College (acceptance no.: SYXK20160006).

Statistical analysis

Statistical analyses were performed using SPSS 22.0 (IBM, SPSS, Chicago, IL, USA) and figures were produced using GraphPad Prism 6.0 or Originpro.9.0. Differences between the different groups were tested using the Student's *t*-test or one-way ANOVA. Kaplan–Meier method was used to evaluate the survival rate and analyzed by log-rank test. The correlations were analyzed using Pearson's correlation coefficients. The univariate and multivariate analyses were analyzed using Cox proportional hazards models. All experimental data were presented as the mean ± S.D. of at least three independent experiments. The differences were considered to be significant at $p < 0.05$.

Author details
[1]General Clinical Research Center, Nanjing First Hospital, Nanjing Medical University, 210006 Nanjing, China. [2]School of Medicine, Southeast University, 210009 Nanjing, China

Conflict of interest
The authors declare that they have no conflict of interest.

Publisher's note
Springer Nature remains neutral with regard to jurisdictional claims in published maps and institutional affiliations.

References

1. Brenner, H., Kloor, M. & Pox, C. P. Colorectal cancer. *Lancet* **383**, 1490–1502 (2014).
2. Dienstmann, R. et al. Consensus molecular subtypes and the evolution of precision medicine in colorectal cancer. *Nat. Rev. Cancer* **17**, 268 (2017).
3. Jeck, W. R. & Sharpless, N. E. Detecting and characterizing circular RNAs. *Nat. Biotechnol.* **32**, 453–461 (2014).
4. Rybak-Wolf, A. et al. Circular RNAs in the mammalian brain are highly abundant, conserved, and dynamically expressed. *Mol. Cell* **58**, 870–885 (2015).
5. Chen, J. et al. Circular RNA profile identifies circPVT1 as a proliferative factor and prognostic marker in gastric cancer. *Cancer Lett.* **388**, 208–219 (2017).
6. Weng, W. et al. Circular RNA ciRS-7-A promising prognostic biomarker and a potential therapeutic target in colorectal cancer. *Clin. Cancer Res.* **23**, 3918–3928 (2017).
7. Jeck, W. R. et al. Circular RNAs are abundant, conserved, and associated with ALU repeats. *RNA* **19**, 141–157 (2013).
8. Liang, D. & Wilusz, J. E. Short intronic repeat sequences facilitate circular RNA production. *Genes Dev.* **28**, 2233–2247 (2014).
9. Shan, K. et al. Circular noncoding RNA HIPK3 mediates retinal vascular dysfunction in diabetes mellitus. *Circulation* **136**, 1629–1642 (2017).
10. Zheng, Q. et al. Circular RNA profiling reveals an abundant circHIPK3 that regulates cell growth by sponging multiple miRNAs. *Nat. Commun.* **7**, 11215 (2016).
11. Li, Y. et al. CircHIPK3 sponges miR-558 to suppress heparanase expression in bladder cancer cells. *EMBO Rep.* **18**, 1646–1659 (2017).
12. Thomson, D. W. & Dinger, M. E. Endogenous microRNA sponges: evidence and controversy. *Nat. Rev. Genet.* **17**, 272–283 (2016).
13. Han, D. et al. Circular RNA circMTO1 acts as the sponge of microRNA-9 to suppress hepatocellular carcinoma progression. *Hepatology* **66**, 1151–1164 (2017).
14. Hsiao, K. Y. et al. Noncoding Effects of Circular RNA CCDC66 Promote Colon Cancer Growth and Metastasis. *Cancer Res.* **77**, 2339–2350 (2017).
15. Memczak, S. et al. Circular RNAs are a large class of animal RNAs with regulatory potency. *Nature* **495**, 333–338 (2013).
16. Chen, L. et al. circRNA_100290 plays a role in oral cancer by functioning as a sponge of the miR-29 family. *Oncogene* **36**, 4551–4561 (2017).
17. Wei, X. et al. Circular RNA profiling reveals an abundant circLMO7 that regulates myoblasts differentiation and survival by sponging miR-378a-3p. *Cell Death Dis.* **8**, e3153 (2017).
18. Hansen, T. B. et al. Natural RNA circles function as efficient microRNA sponges. *Nature* **495**, 384–388 (2013).
19. Lee, Y. H. et al. C-myb Regulates autophagy for pulp vitality in glucose oxidative stress. *J. Dent. Res.* **95**, 430–438 (2016).
20. Pekarcikova, L., Knopfova, L., Benes, P. & Smarda, J. c-Myb regulates NOX1/p38 to control survival of colorectal carcinoma cells. *Cell Signal.* **28**, 924–936 (2016).
21. Liu, Y. C. et al. CircNet: a database of circular RNAs derived from transcriptome sequencing data. *Nucleic Acids Res.* **44**, D209–D215 (2016).
22. Kabir, T. D. et al. A microRNA-7/growth arrest specific 6/TYRO3 axis regulates the growth and invasiveness of sorafenib-resistant cells in human hepatocellular carcinoma. *Hepatology* **67**, 216–231 (2018).
23. Bhere, D. et al. MicroRNA-7 upregulates death receptor 5 and primes resistant brain tumors to caspase-mediated apoptosis. *NeuroOncology* **20**, 215–224 (2017).
24. Cui, Y. X. et al. MicroRNA-7 suppresses the homing and migration potential of human endothelial cells to highly metastatic human breast cancer cells. *Br. J. Cancer* **117**, 89–101 (2017).
25. Gu, D. N. et al. microRNA-7 impairs autophagy-derived pools of glucose to suppress pancreatic cancer progression. *Cancer Lett.* **400**, 69–78 (2017).
26. Suto, T. et al. MicroRNA-7 expression in colorectal cancer is associated with poor prognosis and regulates cetuximab sensitivity via EGFR regulation. *Carcinogenesis* **36**, 338–345 (2015).
27. Hansen, T. B., Kjems, J. & Damgaard, C. K. Circular RNA and miR-7 in cancer. *Cancer Res.* **73**, 5609–5612 (2013).
28. Hanahan, D. & Weinberg, R. A. Hallmarks of cancer: the next generation. *Cell* **144**, 646–674 (2011).
29. Kristensen, L. S., Hansen, T. B., Veno, M. T. & Kjems, J. Circular RNAs in cancer: opportunities and challenges in the field. *Oncogene* **37**, 555–565 (2017).
30. Malaterre, J. et al. Intestinal-specific activatable Myb initiates colon tumorigenesis in mice. *Oncogene* **35**, 2475–2484 (2016).
31. Ramsay, R. G. & Gonda, T. J. MYB function in normal and cancer cells. *Nat. Rev. Cancer* **8**, 523–534 (2008).
32. Zhu, J. et al. Differential expression of circular RNAs in glioblastoma multiforme and its correlation with prognosis. *Transl. Oncol.* **10**, 271–279 (2017).
33. Fu, L. et al. Hsa_circ_0005986 inhibits carcinogenesis by acting as a miR-129-5p sponge and is used as a novel biomarker for hepatocellular carcinoma. *Oncotarget* **8**, 43878–43888 (2017).
34. Zhong, Z., Lv, M. & Chen, J. Screening differential circular RNA expression profiles reveals the regulatory role of circTCF25-miR-103a-3p/miR-107-CDK6 pathway in bladder carcinoma. *Sci. Rep.* **6**, 30919 (2016).
35. Sun, Y. et al. A novel regulatory mechanism of smooth muscle alpha-actin expression by NRG-1/circACTA2/miR-548f-5p axis. *Circ. Res.* **121**, 628–635 (2017).
36. Yu, C. Y. et al. The circular RNA circBIRC6 participates in the molecular circuitry controlling human pluripotency. *Nat. Commun.* **8**, 1149 (2017).
37. Gu, D. N., Huang, Q. & Tian, L. The molecular mechanisms and therapeutic potential of microRNA-7 in cancer. *Expert Opin. Ther. Targets* **19**, 415–426 (2015).
38. Zhao, X. & Guan, J. L. Focal adhesion kinase and its signaling pathways in cell migration and angiogenesis. *Adv. Drug Deliv. Rev.* **63**, 610–615 (2011).
39. Pollak, M. The insulin and insulin-like growth factor family in neoplasia: an update. *Nat. Rev. Cancer* **12**, 159–169 (2012).
40. Pozzi, C. et al. The EGFR-specific antibody cetuximab combined with chemotherapy triggers immunogenic cell death. *Nat. Med.* **22**, 624–631 (2016).
41. Wang, K. et al. A circular RNA protects the heart from pathological hypertrophy and heart failure by targeting miR-223. *Eur. Heart J.* **37**, 2602–2611 (2016).
42. Zeng, K. et al. BRAF V600E mutation correlates with suppressive tumor immune microenvironment and reduced disease-free survival in Langerhans cell histiocytosis. *Oncoimmunology* **5**, e1185582 (2016).